

Hysteresis in Two Dimensional Arrays of Magnetic Nanoparticles

Manish Anand*

*Department of Physics, Bihar National College,
Patna University, Patna-800004, India.*

(Dated: August 28, 2021)

Abstract

We perform computer simulations to probe the magnetic hysteresis in a two-dimensional ($L_x \times L_y$) assembly of magnetic nanoparticles as a function of dipolar interaction strength h_d , temperature T , aspect ratio $A_r = L_y/L_x$, and the applied alternating magnetic field's direction. In the absence of magnetic interaction ($h_d \approx 0$) and thermal fluctuations ($T = 0$ K), the hysteresis follows the Stoner and Wohlfarth model, as expected. For weak dipolar interaction and substantial temperature, the hysteresis has the dominance of superparamagnetic behaviour, irrespective of the applied magnetic field's direction and A_r . Interestingly, the hysteresis curve has all the characteristics of antiferromagnetic interaction dominance for $A_r \leq 6$ and considerable dipolar interaction strength ($h_d > 0.2$), which is independent of applied magnetic direction. When the magnetic field is applied along the system's shorter axis (x -direction), a non-hysteresis straight line is observed with large h_d . In the case of the magnetic field applied along the long axis of the sample (y -direction), ferromagnetic interaction dominates the hysteresis for large h_d and $A_r > 6$. Irrespective of h_d and applied magnetic field's direction, the coercive field $\mu_o H_c$ and remanence M_r are minimal for $A_r \leq 6$ and significant temperature. They are found to increase with h_d when A_r is enormous. Remarkably, the variation of hysteresis loop area E_H as a function of these parameters is the same as that of the coercive field variation. We believe that the concepts presented in this work are relevant in various technological applications such as spintronics and magnetic hyperthermia, in which such self-assembled nanoparticle arrays are ubiquitous.

* itsanand121@gmail.com

I. INTRODUCTION

In recent years, two-dimensional arrays of magnetic nanoparticles (MNPs) have received significant attention due to their unique magnetic properties and potential technological applications [1–8]. From theoretical perspectives, they pose an exciting research topic in which competing interactions, reduced dimensionality, shape anisotropy, etc., lead to novel collective behaviours [9–11]. On the other hand, such systems are ideal candidates for diverse technological applications such as spintronics, high-density data storages, magnetic hyperthermia, etc. [12–17].

The magnetic properties of non-interacting MNPs are well understood [18, 19]. However, they are found to interact in an assembly due to dipolar interaction [20, 21]. The dipolar interaction is long-ranged and anisotropic [22]. Further, it can allow for both ferromagnetic and antiferromagnetic couplings depending on the relative position of MNPs. As a consequence, it has varied effects on systemic properties [23–25]. In some cases, the dipolar interaction causes spins’s frustration, modifies energy barriers, and imparts spin-glass-like properties. When the system size is smaller than the range of dipolar interaction, it can create unconventional spins morphologies. Depending on the lattice structure, there have been observations of magnetic vortices, antiferromagnetic states, checkerboard patterns, etc. [26, 27]. Consequently, they exhibit unusual ground-state and relaxation characteristics. For example, the dipolar interaction elevates the blocking temperature even with weak interaction strength [28]. The dipolar interaction also affects the ground state spins configuration depending on the geometry of the system. In the face-centred cubic arrangement of MNPs, Luttinger *et al.* have found the ground state to be ferromagnetic while it is antiferromagnetic in a simple cubic lattice [29]. The dipolar interaction promotes antiferromagnetic coupling with the square arrangement of MNPs [30, 31]. On the contrary, the dipolar interaction promotes ferromagnetic coupling in the assembly of magnetic moments arranged in triangular lattice [32].

The dipolar interaction also drastically modifies the magnetic properties in such cases [33–38]. For instance, V. Russier studied the magnetic properties, and orientational structure for spherical assembly of MNPs arranged in square and hexagonal lattices at temperature $T = 0$ K [36]. The dipolar interaction is found to induce in-plane orientation of magnetic moments. Xue *et al.* studied the magnetic hysteresis behaviour in a hexagonal array of MNPs with

perpendicular anisotropy [37]. The shape of the hysteresis curve changes from rectangular to a non-hysteresis straight line, increasing dipolar interaction strength. For the triangular arrangement of MNPs, Figueiredo *et al.* observed an increase in the blocking temperature and relaxation time with increased dipolar interaction strength [38]. The dipolar interaction also affects the hysteresis loop area in an assembly of MNPs, one of the most valuable parameters for magnetic hyperthermia applications. Using the molecular dynamics anisotropic diffusion model, Myrovali *et al.* have found the dipolar interaction increases the hysteresis loop area in an assembly of interacting MNPs [39]. Using kinetic Monte Carlo simulation, we have shown that dipolar interaction increases the hysteresis loop area in a one-dimensional chain of MNPs [40]. Using micromagnetic simulations, Haase and Nowak reported that magnetic hyperthermia efficiency decreases with an increase in dipolar interaction strength [41]. The dipolar interaction also has a drastic effect on the tunnel magnetoresistance, a useful quantifier for spintronics based applications [42–46]. For example, Tan *et al.* found the detrimental effect of dipolar interaction on the tunnel magnetoresistance in square arrays of MNPs [44]. Kechrakos *et al.* and Yang *et al.* observed an enhancement in the tunnel magnetoresistance because of dipolar interaction [45, 46].

The above studies clearly suggest that dipolar interaction plays an essential role in determining the magnetic properties of self-assembled MNPs, which are of profound technological importance. However, a systematic study of the effect of dipolar interaction strength, temperature, the shape of the system, and external magnetic field’s direction on the underlying system’s magnetic properties have received little attention in the literature. These studies could provide a concrete theoretical basis in choosing suitable system parameters for various technological applications of interest. In the present work, we perform kinetic Monte Carlo (kMC) simulations to study the magnetic hysteresis in the two-dimensional assembly of MNPs as a function of various parameters of interest. In particular, we perform a detailed study of the dependence of magnetic hysteresis on dipolar interaction strength, temperature, aspect ratio and direction of the applied magnetic field.

This paper is organized as follows. In Sec. II, we present the model for an assembly of MNPs and discuss the kMC simulations briefly. The numerical results will be presented in Sec. III. Finally, we summarize and discuss the main results in Sec. IV.

II. THEORETICAL FRAMEWORK

We consider an assembly of spherical magnetic nanoparticles arranged in a two-dimensional lattice in the xy -plane with system dimension $L_x \times L_y$. The particle has a diameter D , and the lattice spacing is a , as shown in Fig. 1(a). Each particle has a magnetic moment $\mu = M_s V$, M_s being the saturation magnetization, and $V = \pi D^3/6$ is the volume of the nanoparticle. Further, each nanoparticle is assumed to have uniaxial anisotropy $\vec{K} = K_{\text{eff}} \hat{k}$, where K_{eff} is the uniaxial anisotropy constant, and \hat{k} is the direction of anisotropy or easy axis. We have assumed anisotropy axes to be randomly oriented. The energy associated with such nanoparticle due to magnetocrystalline anisotropy is given by [47, 48]

$$E_K = K_{\text{eff}} V \sin^2 \theta \quad (1)$$

Here θ is the angle between anisotropy axis and magnetic moment.

MNPs also interact due to the long-ranged dipolar interaction [49]. We can calculate the dipolar interaction energy E_{dip} in an assembly of MNPs as [50–52]

$$E_{\text{dip}} = \frac{\mu_o}{4\pi a^3} \sum_{j, j \neq i} \left[\frac{\vec{\mu}_i \cdot \vec{\mu}_j}{(r_{ij}/a)^3} - \frac{3(\vec{\mu}_i \cdot \hat{r}_{ij})(\vec{\mu}_j \cdot \hat{r}_{ij})}{(r_{ij}/a)^3} \right]. \quad (2)$$

Here μ_o is the permeability of free space; $\vec{\mu}_i$ and $\vec{\mu}_j$ are the magnetic moment vectors of i^{th} and j^{th} nanoparticle respectively, and r_{ij} is the center-to-center separation between μ_i and μ_j . \hat{r}_{ij} is the unit vector corresponding to \vec{r}_{ij} . The corresponding dipolar field $\mu_o \vec{H}_{\text{dip}}$ is given by the following expression [51, 53]

$$\mu_o \vec{H}_{\text{dip}} = \frac{\mu \mu_o}{4\pi a^3} \sum_{j, j \neq i} \frac{3(\hat{\mu}_j \cdot \hat{r}_{ij})\hat{r}_{ij} - \hat{\mu}_j}{(r_{ij}/a)^3}. \quad (3)$$

As it is clearly evident from Eq. (2) and Eq. (3) that dipolar interaction varies as $1/r_{ij}^3$, we can define the strength of dipolar interaction $h_d = D^3/a^3$ [44]. So $h_d = 1.0$ is the largest dipolar interaction strength, and $h_d = 0$ can be termed as the non-interacting case.

We apply an oscillating magnetic field to probe the hysteresis behaviour of dipolar interacting MNPs. It is given by [40]

$$\mu_o H = \mu_o H_o \cos \omega t, \quad (4)$$

where $\mu_o H_o$ and $\omega = 2\pi\nu$ are the amplitude and angular frequency of the applied magnetic field respectively, ν is the linear frequency, and t is the time. Therefore, the total energy

of the underlying system under the influence of dipolar and external magnetic field is given by [53, 54]

$$E = K_{\text{eff}} V \sum_i \sin^2 \theta_i + \frac{\mu_o \mu^2}{4\pi a^3} \sum_{j, j \neq i} \left[\frac{\hat{\mu}_i \cdot \hat{\mu}_j - 3(\hat{\mu}_i \cdot \hat{r}_{ij})(\hat{\mu}_j \cdot \hat{r}_{ij})}{(r_{ij}/a)^3} \right] - \mu_o \sum_i \vec{\mu}_i \cdot \vec{H} \quad (5)$$

Here θ_i is the angle between the anisotropy axis and the i^{th} magnetic moment of the system.

We implement kMC simulations to probe the hysteresis response as a function of dipolar interaction strength h_d , temperature T , aspect ratio $A_r = L_y/L_x$, and the applied magnetic field's direction. In the kMC algorithm, dynamics is captured more accurately, which is essential to study the dynamic hysteresis response of dipolar interacting MNPs [55]. Using this technique, we can accurately describe the dynamical properties of MNPs in the superparamagnetic or ferromagnetic regime without any artificial or abrupt separation between them [53]. We have used the same algorithm, which is described in greater detail in the work of Tan *et al.* and Anand *et al.* [53, 54]. Therefore, we do not reiterate it here to avoid repetition.

The amount of heat dissipated by the MNPs assembly during one complete cycle of the external magnetic field equals the hysteresis loop area E_H . It can be evaluated using the following formula [33]

$$E_H = \oint M(H) dH, \quad (6)$$

The above intergral is evaluated over the entire period of the external magnetic field change. $M(H)$ is the magnetization of system at magnetic field H .

III. SIMULATIONS RESULTS

We consider spherically shaped nanoparticles of Fe_3O_4 arranged in a two-dimensional lattice ($L_x \times L_y$) with $D = 8$ nm, $K_{\text{eff}} = 13 \times 10^3 \text{ Jm}^{-3}$, and $M_s = 4.77 \times 10^5 \text{ Am}^{-1}$. The total number of nanoparticles in the assembly is considered as $n = 400$. We have considered seven values of system sizes viz. $L_x \times L_y = 20 \times 20, 16 \times 25, 10 \times 40, 8 \times 50, 4 \times 100, 2 \times 200$ and 1×400 . The corresponding aspect ratio $A_r (= L_y/L_x)$ of the underlying system is 1.0, 1.56, 4.0, 6.25, 25, 100 and 400, respectively. The dipolar interaction strength h_d is varied from 0 to 1.0. The temperature T is changed between 0 and 300 K. The anisotropy axes are assumed to have random orientations. The alternating magnetic field is applied along x

and y -direction. The amplitude of the magnetic field strength $\mu_o H_o$ and its frequency ν is taken as 0.10 T and 10^5 Hz, respectively.

First, we study the magnetic hysteresis in a square lattice with $L_x \times L_y = 20 \times 20$. we have considered six representative values of dipolar interaction strength $h_d = 0, 0.2, 0.4, 0.6, 0.8$ and 1.0 . The temperature is taken as 300 K, and the magnetic field is applied along x -direction in Fig. 1(b) and along y -direction in Fig. 1(c). In all the hysteresis curves shown in the present article, the x -axis (applied magnetic field) and y -axis (magnetization) have been scaled by single-particle anisotropy field $H_K = 2K_{\text{eff}}/M_s$ [47] and M_s , respectively. The hysteresis curve has the negligible value of coercive field and remanence for weakly interacting MNPs ($h_d \leq 0.2$) indicating the dominance of superparamagnetic character. Interestingly, the dipolar interaction induces antiferromagnetic coupling for large magnetic interaction strength ($h_d > 0.2$). As a consequence, the corresponding hysteresis curve has all the signatures of the dominance of antiferromagnetic interaction, i.e., zero value of remanence. These observations are in perfect agreement with the work of Chen *et al.* [56]. It is also in qualitative agreement with the work of Ewerlin *et al.* [57]. These observations are also independent of the direction of the applied magnetic field as long it is applied in a plane of the system.

To see the effect of aspect ratio A_r and direction of the applied magnetic field on the hysteresis, we then study magnetic hysteresis for six values of A_r in Fig. (2). The magnetic field is applied along the x -direction, and temperature T is taken as 300 K. Irrespective of A_r , the hysteresis loop area is negligibly tiny for very weak dipolar interaction strength ($h_d \leq 0.2$), indicating the dominance of superparamagnetic behaviour. For large dipolar interaction strength and relatively small aspect ratio $A_r \leq 6.0$, the dipolar interaction induces antiferromagnetic coupling, which is reflected in the negligible value of remanence and coercive field. When the aspect ratio is large ($A_r > 6.0$), we observe non-hysteresis for considerable dipolar interaction strength. We can explain it using the fact that the magnetic moment's natural tendency is to get aligned along the sample's longer axis (along y). The applied magnetic field forces the magnetic moment to aligned along the shorter side of the sample. As a consequence, non-hysteresis is observed for sizeable dipolar interaction strength.

In Fig. (3), we apply the magnetic field along the y -direction. All other parameters are the same as that of Fig. (2). There is a dominance of antiferromagnetic interaction for

considerable dipolar interaction strength ($h_d > 0.2$) and $A_r < 6.0$ in this case also. While for weak dipolar interaction strength, the hysteresis loop area is negligibly small irrespective of A_r , which indicates the signature of superparamagnetic behaviour. Remarkably, the dipolar interaction induces ferromagnetic coupling for $h_d > 0.2$ and a very large aspect ratio ($A_r > 6.0$). Consequently, the coercive field and remanence have huge values and get enhanced with an increase in h_d . One can explain it using the fact that the dipolar interaction forces the magnetic moment to get aligned along the sample's longer axis due to the increased value of shape anisotropy. For extremely large A_r and strongest interacting MNPs ($h_d = 1.0$), remanence is close to 1.0, indicating extremely large ferromagnetic coupling. It is evident that for sizeable dipolar interaction strength, there is a transition point at $A_r \leq 6.0$; below this value, antiferromagnetic coupling dominates. For a larger value of A_r , ferromagnetic coupling prevails. These results suggest that the nature of the interaction can be tuned from antiferromagnetic to ferromagnetic just by changing the aspect ratio provided the dipolar interaction strength is very large. It has got profound applications in spintronics based applications where one needs large tunnel magnetic resistance, which could be maximized with the antiferromagnetic arrangement of MNPs [3]. The latter can thus be achieved for the sample having a smaller aspect ratio and sizeable dipolar interaction.

Temperature also plays an essential role in determining the magnetic hysteresis response in an array of dipolar interacting MNPs. So, now we study the temperature dependence of hysteresis for various aspect ratio and the applied magnetic field direction. In Fig. (4), we plot the hysteresis curve for the square sample ($L_x \times L_y = 20 \times 20$) with various values of T for weakly interacting MNPs ($h_d = 0.2$). The magnetic field is applied along the x -direction. In the absence of thermal fluctuations ($T = 0$ K), the system behaves like a blocked state. The corresponding hysteresis curve shows the coercive field value of $0.48H_K$ and remanence ~ 0.5 , which are in perfect agreement with the Stoner and Wohlfarth model [58]. It is also in qualitative agreement with the work of V. Russier [36]. There is a decrease in the hysteresis loop area with an increase in temperature. It can be explained using the fact the with an increase in thermal fluctuations; magnetic moments tends to orient randomly, resulting in the minimal value of coercive field and remanence provided the dipolar interaction strength is weak. These observations are robust with respect to the aspect ratio and direction of the applied magnetic field. Therefore curves are not shown for other values of A_r and direction of the applied magnetic field to avoid duplications.

In the case of sizeable dipolar interaction strength, the hysteresis response should depend on the direction of the applied magnetic field and aspect ratio for a given temperature. Therefore, we study the magnetic hysteresis with $h_d = 0.4$ as a function of temperature for three representative values of aspect ratio $A_r = 1.0, 1.56$ and 100 in Fig. (5). T is varied between 0 to 300 K and the magnetic field along x and y -direction. For small A_r and $T > 20$ K, antiferromagnetic interaction is dominant resulting in negligible remanence and the coercive field value. The system tends to behave as a blocked state for the small value of T . These observations are independent of applied magnetic field's direction. On the other hand, in the case of huge aspect ratio, the hysteresis curve depends strongly on the applied magnetic field's direction. The hysteresis loop area is very small when the field is applied along the x -direction. The dipolar interaction induces ferromagnetic coupling when the field is applied along the long axis of the sample (y -direction), which results in a tremendous value of coercive field and remanence. Consequently, the hysteresis loop area is very large compared to the field applied along the sample's shorter axis (x -direction). The hysteresis loop decreases with an increase in temperature because of enhancement in thermal fluctuations.

To see further the effect of temperature on the hysteresis for enormous dipolar interaction strength, we plot magnetic hysteresis curves for $h_d = 0.6$ and 0.8 in Fig. (6) and Fig. (7), respectively. All other parameters are the same as that of Fig. (5). Irrespective of the applied magnetic field's direction, the hysteresis curve shows the dominance of antiferromagnetic interaction for a small value of $A_r (\leq 6.0)$. The hysteresis curve has a negligibly small value of the coercive field and remanence when the magnetic field is applied along the sample's shorter axis (x -axis). It is due to the fact that the natural tendency of magnetic moments is to get aligned along the long axis of the sample; the applied magnetic field along x -direction forces them to orient along the system's shorter axis, which results in a minimal hysteresis loop area. In the case of the magnetic field applied along the long axis of the sample (y -axis), the hysteresis loop area is huge, indicating the ferromagnetic coupling dominance. As the dipolar interaction strength is very large, the temperature does not affect the hysteresis behaviour irrespective of the applied magnetic field's direction.

In Fig. (8), we study the temperature dependence of hysteresis for the strongest dipolar interacting MNPs ($h_d = 1.0$). All other parameters are the same as that of Fig. (7). The hysteresis curve has a negligible value of hysteresis loop area irrespective of the applied mag-

netic field's direction for $A_r \leq 6.0$. We observe a non-hysteresis straight line for A_r 's very large value with the applied field is along the shorter side of the sample(x -direction). Remarkably, the hysteresis shows the dominance of ferromagnetic interaction for an extremely large value of A_r when the field is applied along the long axis of the system. In this case, the hysteresis loop area is enormous. The extremely large value of remanence (~ 1.0) also strengthens the fact the ferromagnetic coupling is the maximum. Temperature does not have an impact on the hysteresis as dipolar interaction strength is the largest in this case.

To quantify the magnetic hysteresis, we now study the variation of coercive field $\mu_o H_c$ (scaled by H_K), remanence M_r and hysteresis loop area E_H as a function of aspect ratio A_r and dipolar interaction strength h_d in Fig. (9). The magnetic field is applied along the y -direction and temperature is taken as $T = 300$ K. The coercive field and remanence are negligibly small for weakly interacting MNPs and small value of A_r indicating the dominance of superparamagnetic behaviour. The antiferromagnetic coupling between the magnetic moment is favoured for large h_d and small values of A_r , which is manifested in the minimal value of M_r and $\mu_o H_c$. On the other hand, there is an enhancement in the coercive field and remanence magnetization with an increase in dipolar interaction strength for large A_r , indicating the ferromagnetic coupling dominance. When the dipolar interaction strength and aspect ratio are enormous, there is weak dependence of coercive field and remanence on A_r . Remarkably, the variation of E_H with aspect ratio and dipolar interaction strength is precisely similar to that of coercive field variation. Our results for $h_d = 0$ is in perfect agreement with the works of Carrey *et al.* [47]. We could not compare the entire range of aspect ratio and h_d as they have concentrated only on the non-interacting case ($h_d = 0$). Therefore, our results can be used as a benchmark in this context. These results could be used for choosing correct values of dipolar interaction strength, aspect ratio for optimizing heat dissipation and tunnel magnetoresistance for magnetic hyperthermia and spintronics based applications.

Finally, we study the variation of coercive field and remanence as a function of dipolar interaction strength and temperature for various values of aspect ratio. In Fig. (10), we plot the variation of $\mu_o H_c$ (scaled by H_K) and M_r as a function of T and h_d for three representative values of aspect ratio $A_r = 1.0, 1.56$ and 100 . The coercive field and remanence magnetization are negligibly small irrespective of h_d and T for square sample. In the case of weak dipolar interaction and a large value of temperature, the coercive field and rema-

nence have minimal values, which indicates the dominance of superparamagnetic character. The results with square sample is in qualitative agreement with the work of Figueiredo *et al.* [38]. We could not compare for other aspect ratio as they have concentrated on square geometry. It is also in qualitative agreement with the work of Ewerlin *et al.* [57]. While for large dipolar interaction strength, there is a negligible value of remanence and coercive field as the antiferromagnetic coupling is dominant in this case. Similar observations can be made for $A_r = 1.56$ except at smaller dipolar interaction strength and temperature values where remanence and coercive field is higher. Remarkably, the coercive field and remanence increase with an increase in h_d for a given temperature, provided the aspect ratio is huge. It is because of the enhanced ferromagnetic coupling. In the case of extremely large value of dipolar interaction strength, coercive field and remanence magnetization are very large and they depend very weakly on the temperature. The variation of E_H with T and h_d is also found to be the same as that of coercive field variation. Therefore we have not shown the corresponding curves of E_H variation.

IV. SUMMARY AND CONCLUSION

Now we summarize and discuss the main results of the present work. We have used kinetic Monte Carlo simulation technique to study the magnetic hysteresis in a two-dimensional arrangement of MNPs. We have systematically probed the hysteresis response as a function of dipolar interaction strength h_d , system size ($L_x \times L_y$) or the aspect ratio A_r , temperature T and direction of the applied magnetic field. In the absence of thermal fluctuations and negligible dipolar interaction, the hysteresis curve obeys the Stoner and Wohlfarth model irrespective of aspect ratio and direction of the applied magnetic field. The superparamagnetic behaviour is dominant for weak dipolar interaction strength and large value of temperature, manifested in the minimal hysteresis loop area. Interestingly, the dipolar interaction is found to induce antiferromagnetic coupling provided the aspect ratio A_r is relatively small (≤ 6.0) and $h_d \geq 0.2$, irrespective of the direction of the applied magnetic field. Therefore, the corresponding hysteresis curve shows a negligible value of remanence and coercive field [57]. On the other hand, for large dipolar interaction strength and A_r , the ferromagnetic coupling is dominant with the magnetic field applied the sample's longer axis (y -direction). Temperature is also found to affect the hysteresis properties of the underlying system. In the case of

weak dipolar interaction, the system moves from the blocked state to a superparamagnetic state as the temperature is increased. On the other hand, the temperature does not affect the hysteresis mechanism for large dipolar interaction strength.

The coercive field $\mu_o H_c$, remanence M_r and hysteresis loop area E_H are also useful quantifier to analyse the hysteresis properties of dipolar interacting MNPs. In the case of negligible and weak dipolar interaction, $\mu_o H_c$ and M_r are extremely small with a large value of temperature, irrespective of A_r and direction of the applied magnetic field. We can interpret it due to the dominance of superparamagnetic behaviour. Remarkably, the dipolar interaction is found to induce antiferromagnetic coupling between the magnetic moments for $h_d > 0.2$ and small values of A_r (≤ 6.0). As a consequence, the corresponding hysteresis curves have negligibly small values of M_r and $\mu_o H_c$. When the magnetic field is applied along the long axis of the sample, there is an increase in coercive field and remanence with an increase in dipolar interaction strength for large A_r , indicating the ferromagnetic coupling dominance. In the case of weak dipolar interaction, $\mu_o H_c$ and M_r decrease with an increase in temperature because of enhancement in thermal fluctuations. While for large dipolar interaction strength, they depend weakly on temperature. Remarkably, There is an intimate relationship between E_H and $\mu_o H_c$ as the variation of E_H with h_d , T and A_r is found to be the same as that coercive field variation.

In conclusion, we analysed the hysteresis properties in a two-dimensional assembly of dipolar interacting MNPs using kinetic Monte Carlo simulations. Our results suggest that the dipolar interaction affects the hysteresis mechanism drastically in such an array of MNPs. Interestingly, the nature of interaction can be tuned by varying the aspect ratio and direction of the applied magnetic field. We believe that these results are extremely useful for spintronics based applications. The observation made in the present article should help the experimentalists to manipulate the hysteresis response and other useful properties of interacting MNPs in a more controlled manner. These results should also be taken into account in interpreting of the experiments and efficient usage of magnetic hyperthermia. Therefore, we hope that the present work could pave the way for joint efforts in experimental, theoretical, and computational studies for these extremely useful and versatile systems.

[1] D. Gallina and G. Pastor, Physical Review X **10**, 021068 (2020).

- [2] B. Alkadour, B. Southern, J. Whitehead, and J. van Lierop, *Physical Review B* **100**, 094416 (2019).
- [3] A. Bupathy, V. Banerjee, and J. Carrey, *Physical Review B* **100**, 064420 (2019).
- [4] Z. Wang and E. Luijten, *Physical Review Letters* **123**, 096101 (2019).
- [5] N. Leo, S. Hohenstein, D. Schildknecht, O. Sendetskyi, H. Luetkens, P. M. Derlet, V. Scagnoli, D. Lançon, J. R. Mardegan, T. Prokscha, *et al.*, *Nature Communications* **9**, 1 (2018).
- [6] T. Wang, Y. Wang, Y. Fu, T. Hasegawa, T. Washiya, H. Saito, S. Ishio, F. Li, H. Oshima, K. Itoh, *et al.*, *Applied Physics Letters* **92**, 192504 (2008).
- [7] Y. Takagaki, C. Herrmann, and E. Wiebicke, *Journal of Physics: Condensed Matter* **20**, 225007 (2008).
- [8] D. Kechrakos and K. Trohidou, *Applied Physics Letters* **81**, 4574 (2002).
- [9] V. F. Puentes, P. Gorostiza, D. M. Aruguete, N. G. Bastus, and A. P. Alivisatos, *Nature Materials* **3**, 263 (2004).
- [10] A. Fraerman and M. Sapozhnikov, *Physical Review B* **65**, 184433 (2002).
- [11] A. Farhan, P. Derlet, A. Kleibert, A. Balan, R. Chopdekar, M. Wyss, L. Anghinolfi, F. Nolting, and L. J. Heyderman, *Nature Physics* **9**, 375 (2013).
- [12] D. P. Valdés, E. Lima, R. D. Zysler, G. F. Goya, E. De Biasi, *et al.*, *Physical Review Applied* **15**, 044005 (2021).
- [13] N. A. Frey and S. Sun, *Inorganic Nanoparticles: Synthesis, Application, and Perspective*, 33 (2010).
- [14] A. Sarella, A. Torti, M. Donolato, M. Pancaldi, and P. Vavassori, *Advanced Materials* **26**, 2384 (2014).
- [15] S. Karmakar, S. Kumar, R. Rinaldi, and G. Maruccio, in *Journal of Physics: Conference Series*, Vol. 292 (IOP Publishing, 2011) p. 012002.
- [16] Z. Mohammadpour and K. Majidzadeh-A, *ACS Biomaterials Science & Engineering* **6**, 1852 (2020).
- [17] Y. Takagaki and K. Ploog, *Physical Review B* **71**, 184439 (2005).
- [18] N. Usov, *Journal of Applied Physics* **107**, 123909 (2010).
- [19] R. Fu, Y. Yan, C. Roberts, Z. Liu, and Y. Chen, *Scientific Reports* **8**, 1 (2018).
- [20] J. G. Ovejero, D. Cabrera, J. Carrey, T. Valdivielso, G. Salas, and F. J. Teran, *Physical Chemistry Chemical Physics* **18**, 10954 (2016).

- [21] Z. Zhao and C. Rinaldi, The Journal of Physical Chemistry C **122**, 21018 (2018).
- [22] G. Barrera, P. Allia, and P. Tiberto, Nanoscale **13**, 4103 (2021).
- [23] H. Kachkachi, A. Ezzir, M. Nogues, and E. Tronc, The European Physical Journal B **14**, 681 (2000).
- [24] M. Anand, Journal of Magnetism and Magnetic Materials **522**, 167538 (2021).
- [25] M. Plumer, J. van Lierop, B. Southern, and J. Whitehead, Journal of Physics: Condensed Matter **22**, 296007 (2010).
- [26] U. Löw, V. Emery, K. Fabricius, and S. Kivelson, Physical Review Letters **72**, 1918 (1994).
- [27] E. Edlund and M. N. Jacobi, Physical Review Letters **105**, 137203 (2010).
- [28] W. Luo, S. R. Nagel, T. Rosenbaum, and R. Rosensweig, Physical Review Letters **67**, 2721 (1991).
- [29] J. Luttinger and L. Tisza, Physical Review **70**, 954 (1946).
- [30] A. MacIsaac, J. Whitehead, K. De’Bell, and P. Poole, Physical Review Letters **77**, 739 (1996).
- [31] K. De’Bell, A. MacIsaac, I. Booth, and J. Whitehead, Physical Review B **55**, 15108 (1997).
- [32] P. Politi, M. G. Pini, and R. Stamps, Physical Review B **73**, 020405 (2006).
- [33] M. Anand, J. Carrey, and V. Banerjee, Physical Review B **94**, 094425 (2016).
- [34] G. T. Landi, Physical Review B **89**, 014403 (2014).
- [35] M. Anand, arXiv preprint arXiv:2101.03356 (2021).
- [36] V. Russier, Journal of Applied Physics **89**, 1287 (2001).
- [37] D. Xue and Z. Yan, Journal of Applied Physics **100**, 103906 (2006).
- [38] W. Figueiredo and W. Schwarzacher, Journal of Physics: Condensed Matter **19**, 276203 (2007).
- [39] E. Myrovali, N. Maniotis, A. Makridis, A. Terzopoulou, V. Ntomprougkidis, K. Simeonidis, D. Sakellari, O. Kalogirou, T. Samaras, R. Salikhov, *et al.*, Scientific Reports **6**, 1 (2016).
- [40] M. Anand, Journal of Applied Physics **128**, 023903 (2020).
- [41] C. Haase and U. Nowak, Physical Review B **85**, 045435 (2012).
- [42] C. Black, C. Murray, R. Sandstrom, and S. Sun, Science **290**, 1131 (2000).
- [43] R. Tan, J. Carrey, C. Desvaux, L.-M. Lacroix, P. Renaud, B. Chaudret, and M. Respaud, Physical Review B **79**, 174428 (2009).
- [44] R. Tan, J. Lee, J. Cho, S. Noh, D. Kim, and Y. Kim, Journal of Physics D: Applied Physics **43**, 165002 (2010).

- [45] D. Kechrakos and K. Trohidou, *Journal of Nanoscience and Nanotechnology* **8**, 2929 (2008).
- [46] Y. Yang, S. Shen, Q. Ye, L. Lin, and Z. Huang, *Journal of Magnetism and Magnetic Materials* **303**, e312 (2006).
- [47] J. Carrey, B. Mehdaoui, and M. Respaud, *Journal of Applied Physics* **109**, 083921 (2011).
- [48] M. Anand, J. Carrey, and V. Banerjee, *Journal of Magnetism and Magnetic Materials* **454**, 23 (2018).
- [49] L. Pei, S. Xuan, J. Wu, L. Bai, and X. Gong, *Langmuir* **35**, 12158 (2019).
- [50] S. Odenbach and S. Thurm, in *Ferrofluids* (Springer, 2002) pp. 185–201.
- [51] R. E. Rosensweig, *Ferrohydrodynamics* (Courier Corporation, 2013).
- [52] N. Usov, O. Serebryakova, and V. Tarasov, *Nanoscale Research Letters* **12**, 1 (2017).
- [53] R. Tan, J. Carrey, and M. Respaud, *Physical Review B* **90**, 214421 (2014).
- [54] M. Anand, V. Banerjee, and J. Carrey, *Physical Review B* **99**, 024402 (2019).
- [55] R. Chantrell, N. Walmsley, J. Gore, and M. Maylin, *Physical Review B* **63**, 024410 (2000).
- [56] B. Chen, H. Xu, C. Ma, S. Mattauch, D. Lan, F. Jin, Z. Guo, S. Wan, P. Chen, G. Gao, *et al.*, *Science* **357**, 191 (2017).
- [57] M. Ewerlin, D. Demirbas, F. Brüssing, O. Petravic, A. A. Ünal, S. Valencia, F. Kronast, and H. Zabel, *Physical Review Letters* **110**, 177209 (2013).
- [58] E. C. Stoner and E. Wohlfarth, *Philosophical Transactions of the Royal Society of London. Series A, Mathematical and Physical Sciences* **240**, 599 (1948).

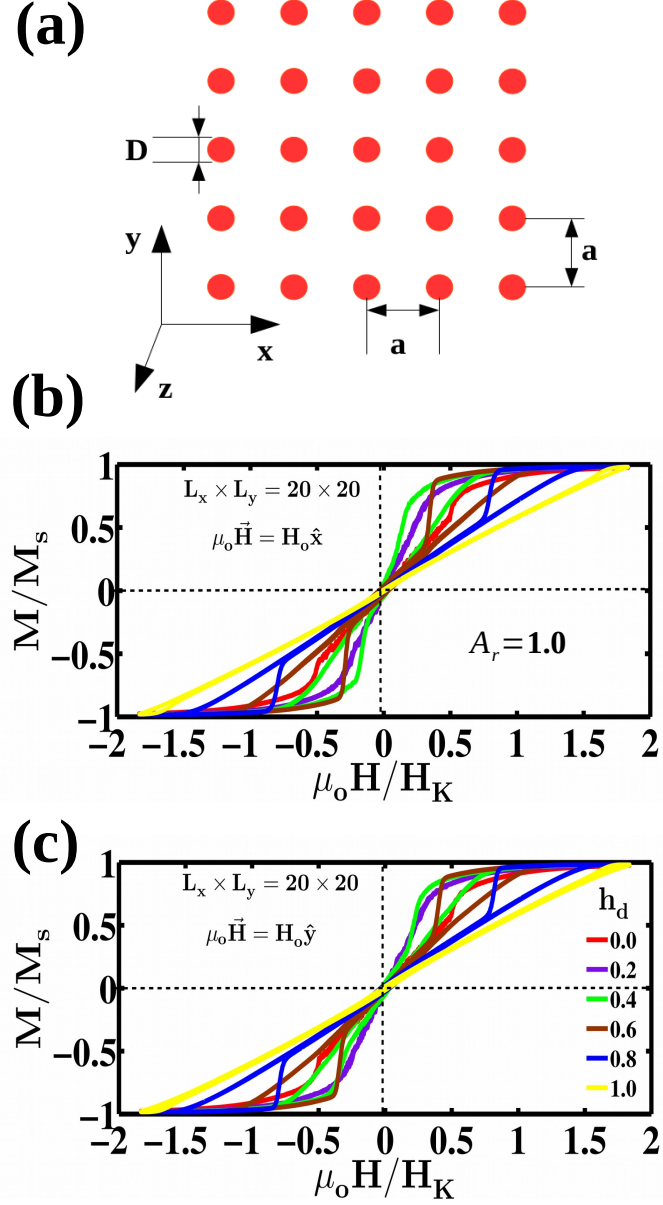


FIG. 1. (a) Schematic of the two-dimensional assembly of MNPs used in the present work, D is the particle diameter and a the lattice spacing. (b) Magnetic hysteresis curves for MNPs arranged in a square lattice as a function of dipolar interaction strength at $T = 300$ K. The external alternating magnetic field is applied along x -direction [(b)] and y -direction [(c)] at $T = 300$ K. For non-interacting and weakly interacting MNPs ($h_d \leq 0.2$), the hysteresis loop area is minimal, indicating the dominance of superparamagnetic behaviour. Interestingly, the hysteresis curve has all the antiferromagnetic interaction characteristics for considerable dipolar interaction strength ($h_d > 0.2$). The hysteresis response is independent of the applied magnetic field's direction (in-plane) in a square lattice.

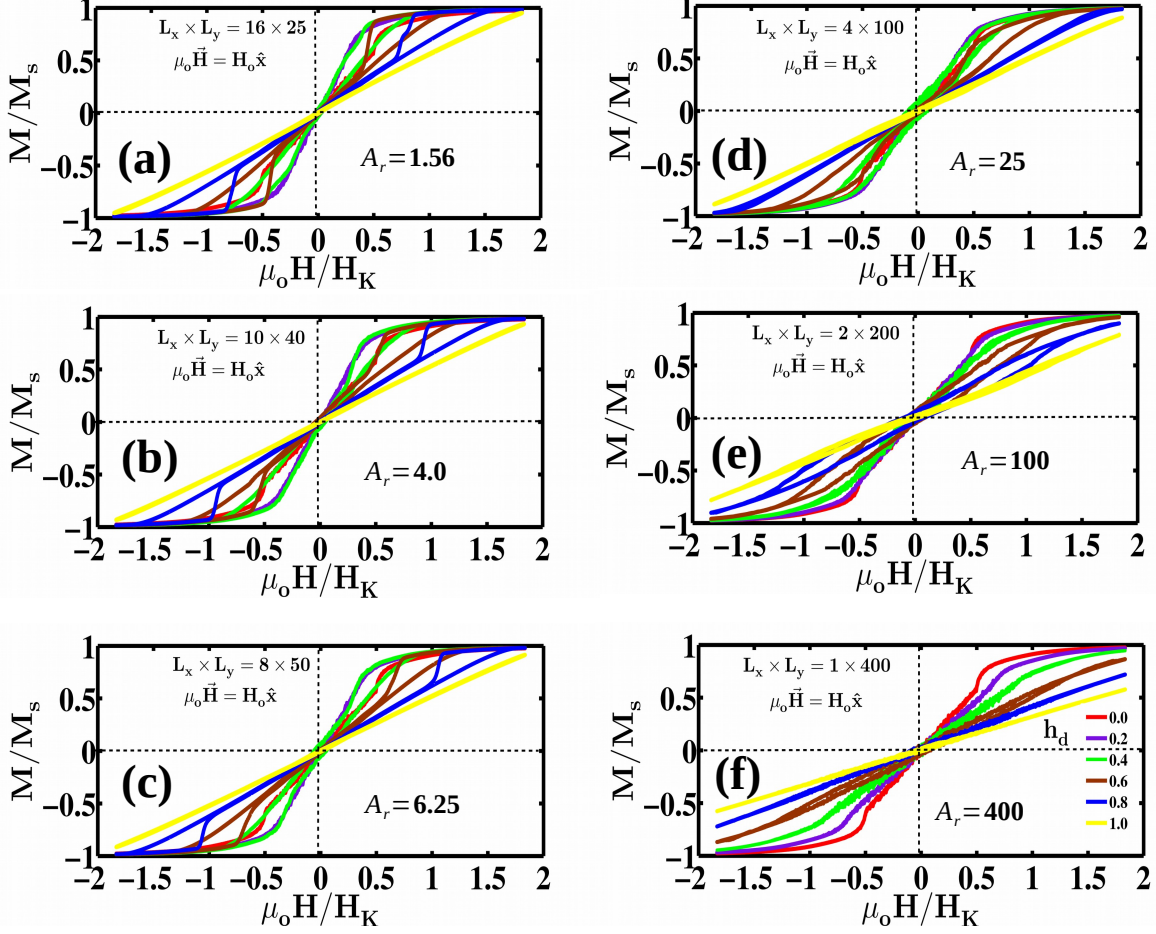


FIG. 2. Magnetic hysteresis curves as a function of dipolar interaction for six values of aspect ratio $A_r = 1.56$ [(a)], 4.0 [(b)], 6.25 [(c)], 25.0 [(d)], 100 [(e)], and 400 [(f)] at $T = 300$ K. The dipolar interaction strength h_d is varied from 0 to 1.0 and the alternating magnetic field is applied along the x -direction. There is a negligible hysteresis loop area with small h_d , which indicates the dominance of superparamagnetic behaviour. For large dipolar interaction strength and $A_r \leq 6.25$, the hysteresis curve has a negligible value of remanence and coercive field, which indicates the dominance of antiferromagnetic coupling. Non-hysteresis is observed for extremely large aspect ratio ($A_r > 6.25$) and dipolar interaction strength $h_d > 0.8$.

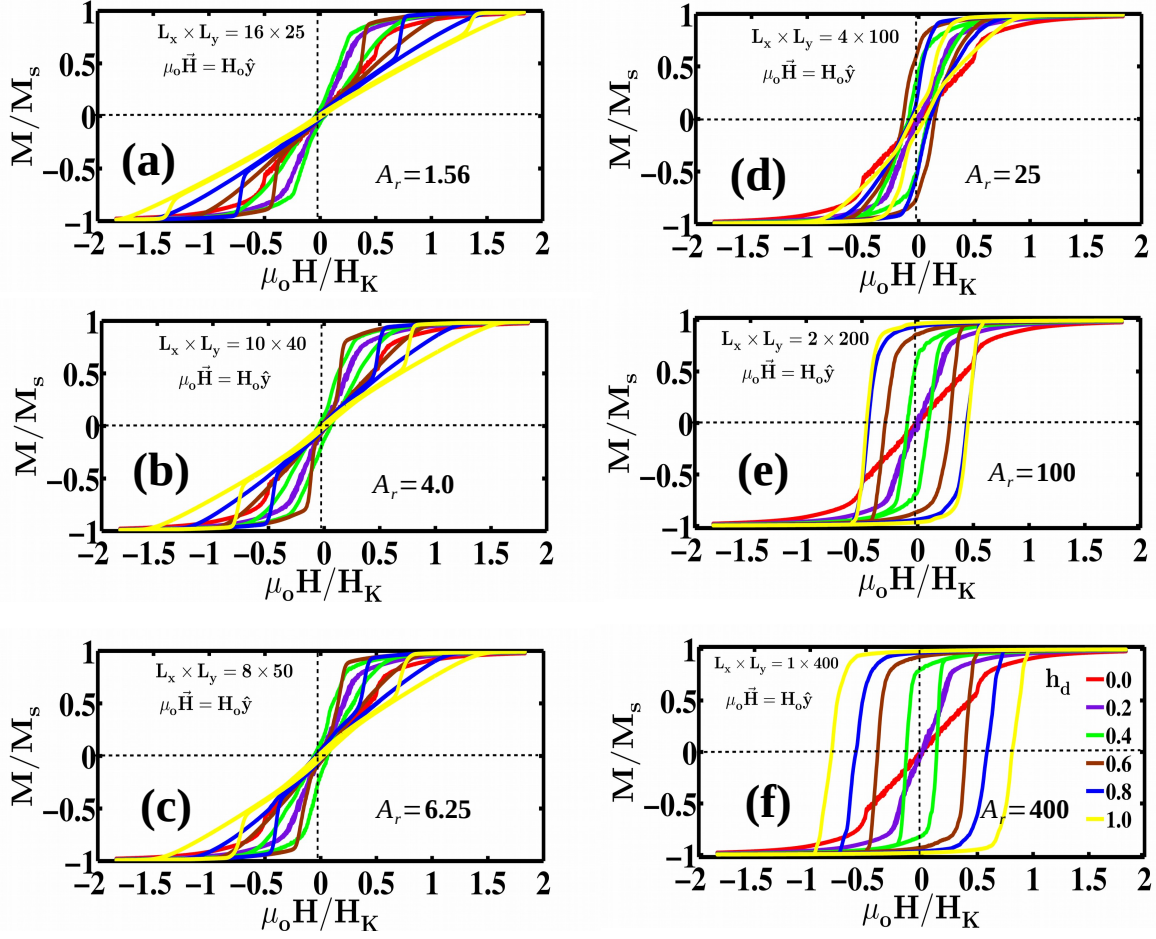


FIG. 3. Magnetic hysteresis curves as a function of dipolar interaction strength h_d with the magnetic field is applied along the y -direction, and $T = 300$ K. We have considered six values of aspect ratio $A_r = 1.56$ [(a)], 4.0 [(b)], 6.25 [(c)], 25.0 [(d)], 100 [(e)], and 400 [(f)]. For $A_r \leq 6.25$ and large dipolar interaction strength h_d , antiferromagnetic interaction dominates the magnetic hysteresis, i.e., the negligible remanence value. Interestingly for large aspect ratio and appreciable dipolar interaction strength, the hysteresis curve has a very large value of coercive field, and remanence. They get enhanced with an increase in h_d . These observations indicate the dominance of ferromagnetic interaction.

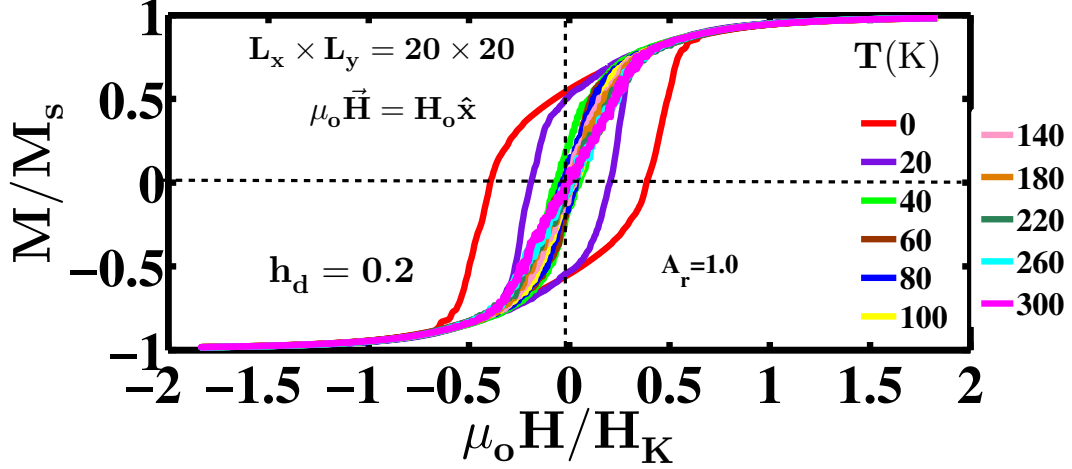


FIG. 4. Magnetic hysteresis curve as a function of temperature T in a square arrangement of MNPs ($A_r = 1.0$) for weakly dipolar interacting ($h_d = 0.2$). The alternating magnetic field is applied along the x -direction. In the absence of thermal fluctuations ($T = 0$ K), the hysteresis curve has the coercive field $\mu_o H_c \sim 0.48 H_K$ and remanence $M_r \sim 0.5$ as expected, which is in perfect agreement with the Stoner and Wohlfarth model. The hysteresis loop area decreases with an increase in temperature because of enhancement in thermal fluctuations. These observations are independent of applied magnetic field's direction (in-plane) and the aspect ratio A_r (curves not shown).

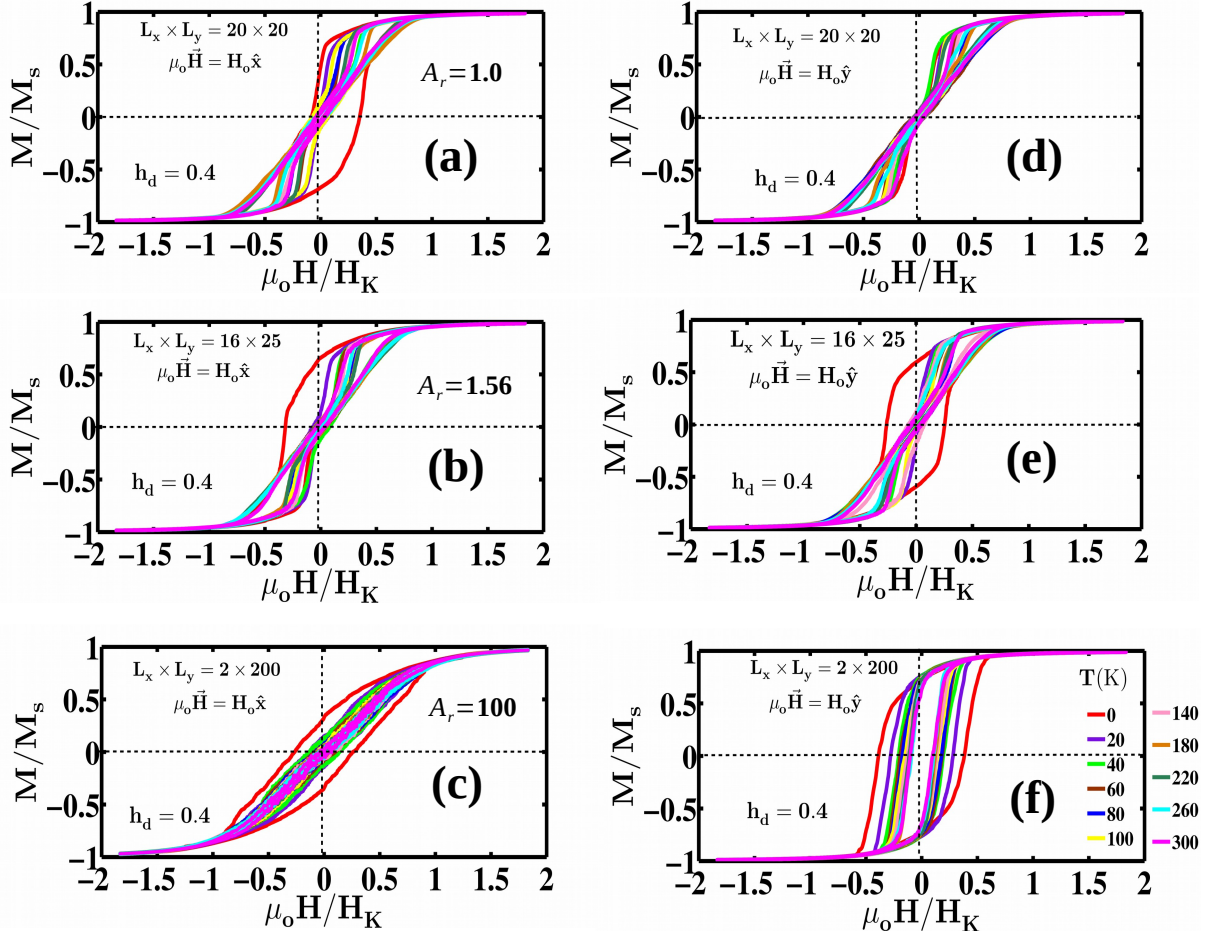


FIG. 5. Magnetic hysteresis curve as a function of temperature T for moderate dipolar interaction ($h_d = 0.4$) and three representative values of aspect ratio $A_r = 1.0, 1.56$ and 100 . The magnetic field is applied along x -direction [(a), (b) and (c)] and y -direction [(d), (e) and (f)]. In the case of small A_r and non-zero temperature, antiferromagnetic interaction is dominant resulting in negligible remanence and coercive field, which is independent of direction of the applied magnetic field. While for large A_r , the hysteresis curve has small hysteresis loop area with the field applied along the shorter axis of the sample (x -direction). Interestingly, there is a large coercive field and remanence with the magnetic field applied along y -direction and A_r is very large, which indicates the dominance of ferromagnetic coupling. There is always a decrease in hysteresis loop area with temperature.

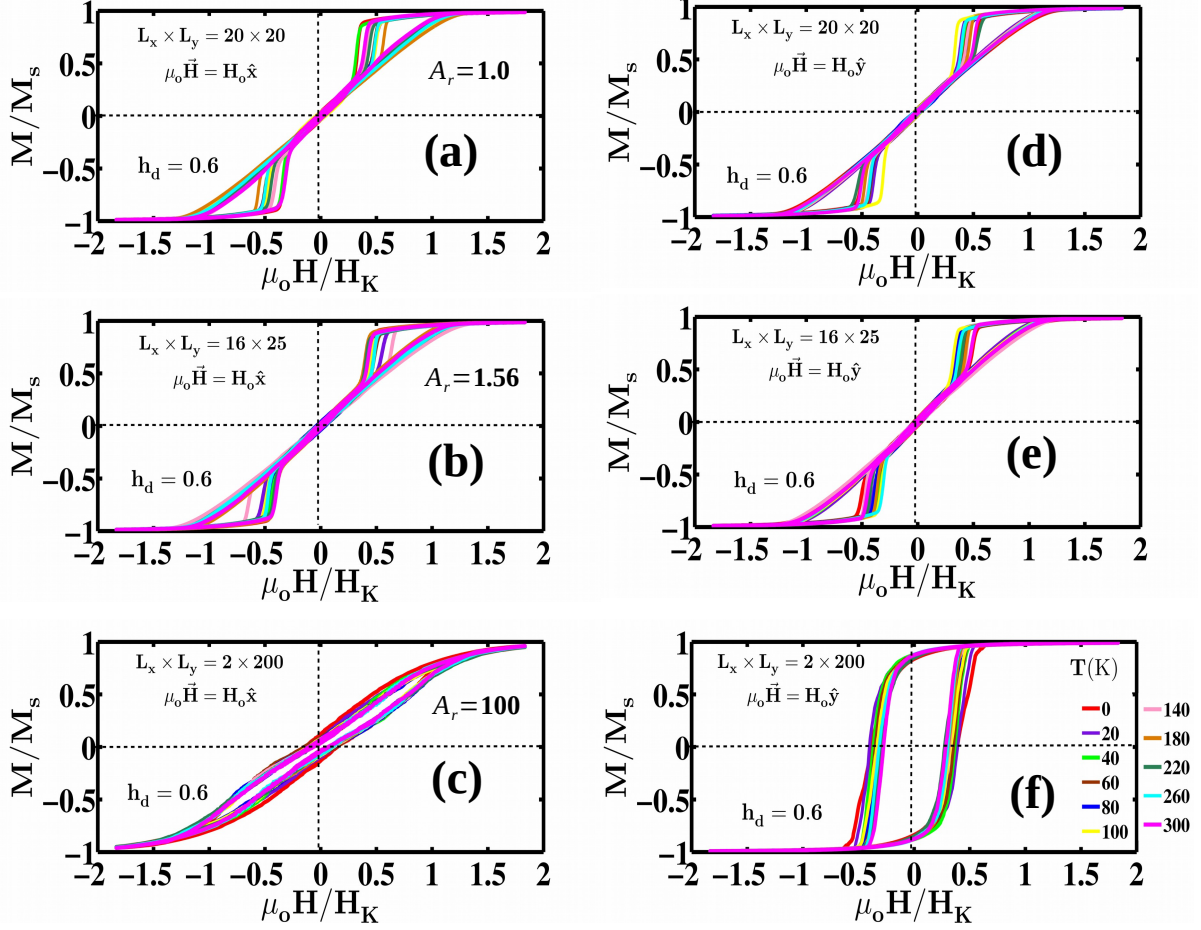


FIG. 6. Temperature dependence of magnetic hysteresis curve with large dipolar interaction $h_d = 0.6$. We have considered three typical values of aspect ratio $A_r = 1.0, 1.56$ and 100 . The magnetic field is applied along x -direction [(a), (b) and (c)] and y -direction [(d), (e) and (f)]. Irrespective of the applied magnetic field's direction, the hysteresis curve has all the characteristics of antiferromagnetic interaction for small A_r . There is a large hysteresis loop area with the magnetic field applied along the sample's long axis (y -direction) and extremely large A_r . There is a weak dependence of hysteresis on temperature.

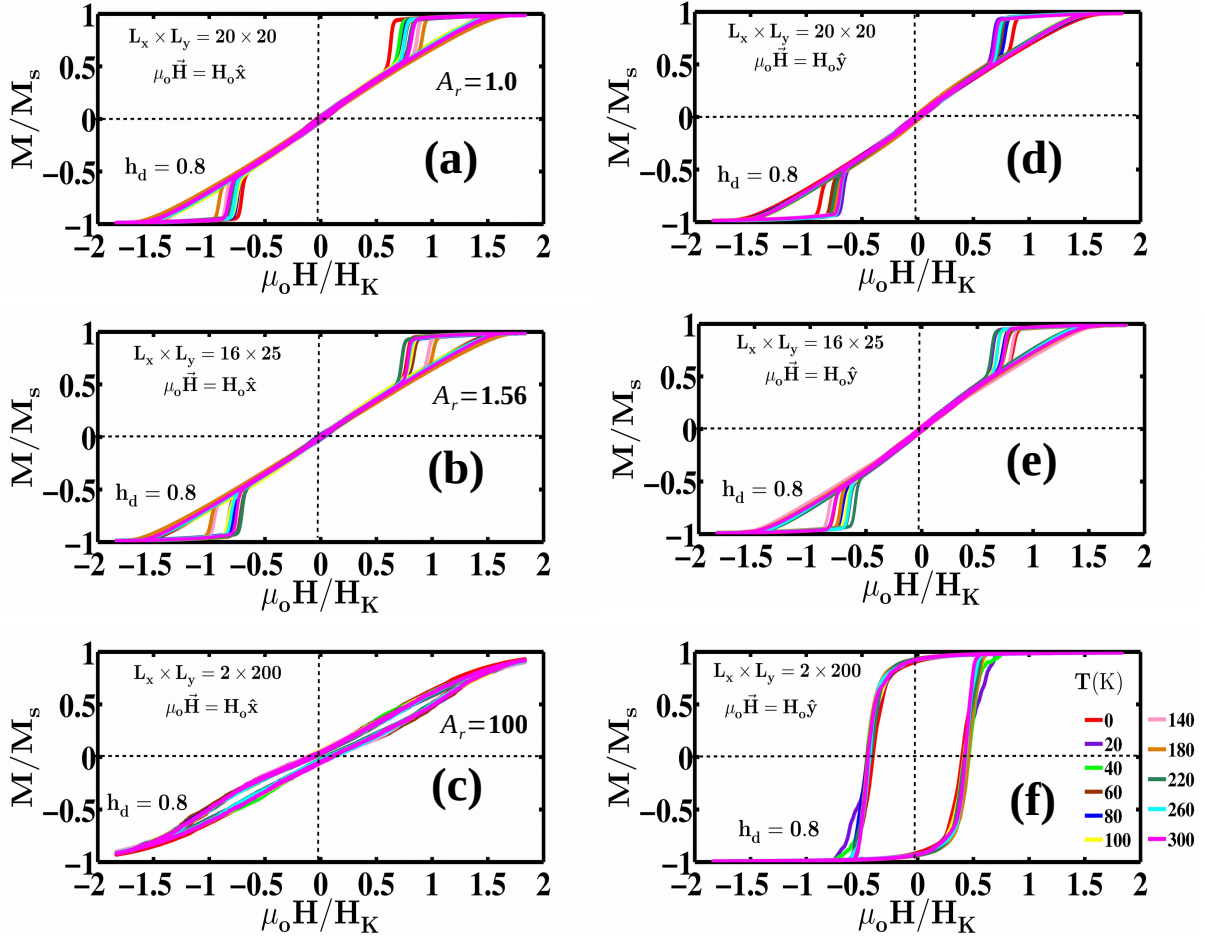


FIG. 7. Magnetic hysteresis as a function of temperature for very large dipolar interaction strength $h_d = 0.8$. We have considered there representative values of $A_r = 1.0$, 1.56 and 100; the magnetic field is applied along x -direction [(a), (b) and (c)] and y -direction [(d), (e) and (f)]. In the case of small A_r and irrespective of applied magnetic field's direction, the hysteresis curve has negligible remanence and the coercive field, indicating the dominance of antiferromagnetic coupling. The hysteresis loop area is minimal with the magnetic field applied along the sample's shorter axis (x -direction), provided the aspect ratio is huge. The hysteresis loop area is very large when the direction of the applied magnetic field is along the longer axis of the system (y -direction) and A_r is enormous.

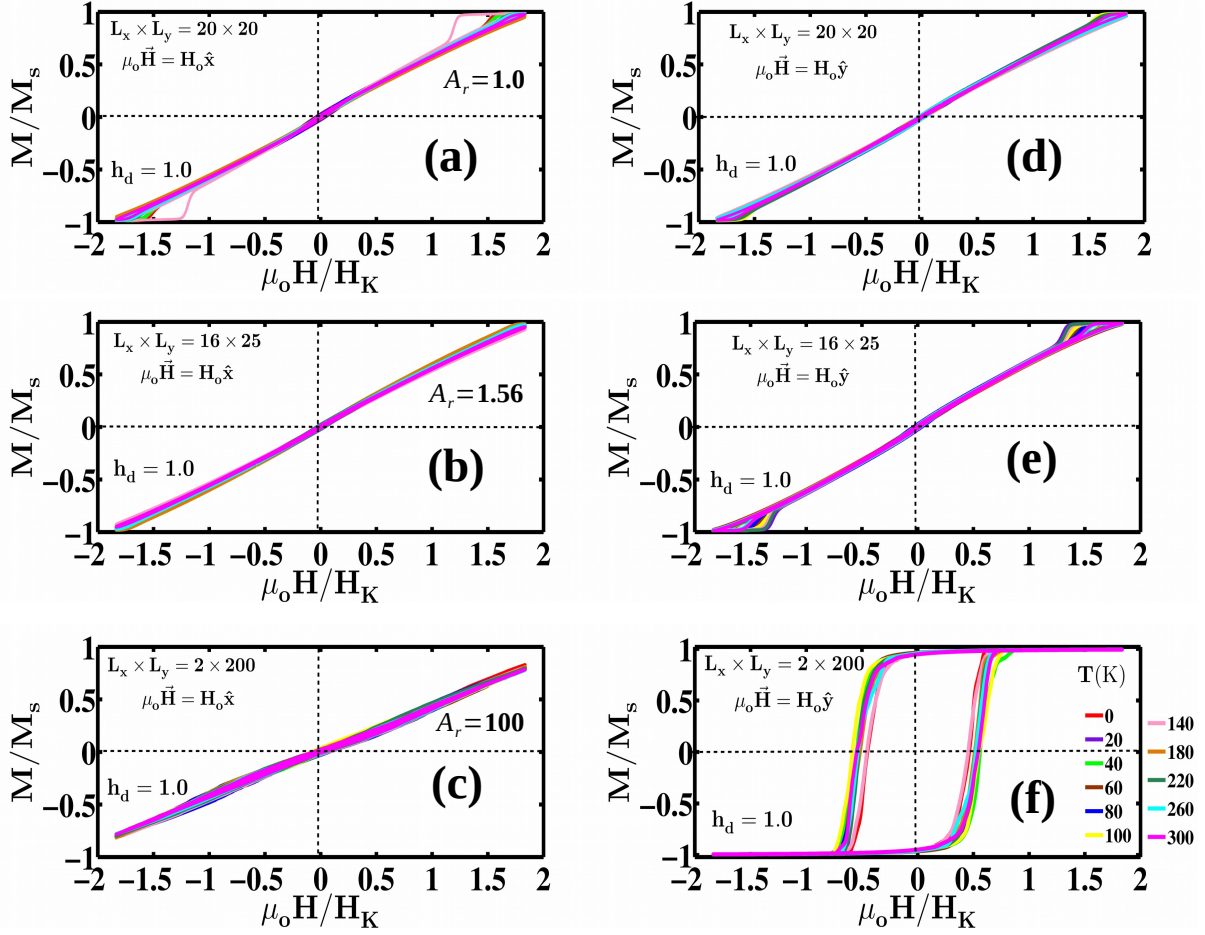


FIG. 8. Magnetic hysteresis curves as a function of temperature for the strongest dipolar interacting MNPs ($h_d = 1.0$) with three values of $A_r = 1.0$, 1.56 and 100 . The magnetic field is applied along x -direction [(a), (b) and (c)] and y -direction [(d), (e) and (f)]. In the case of the magnetic field applied along the x -direction, non-hysteresis is observed irrespective of aspect ratio. The hysteresis loop area is huge, indicating the dominance of ferromagnetic interaction when the field is applied to the longer axis of the sample, provided the aspect ratio is enormous. Temperature does not affect the hysteresis because of substantial large dipolar interaction.

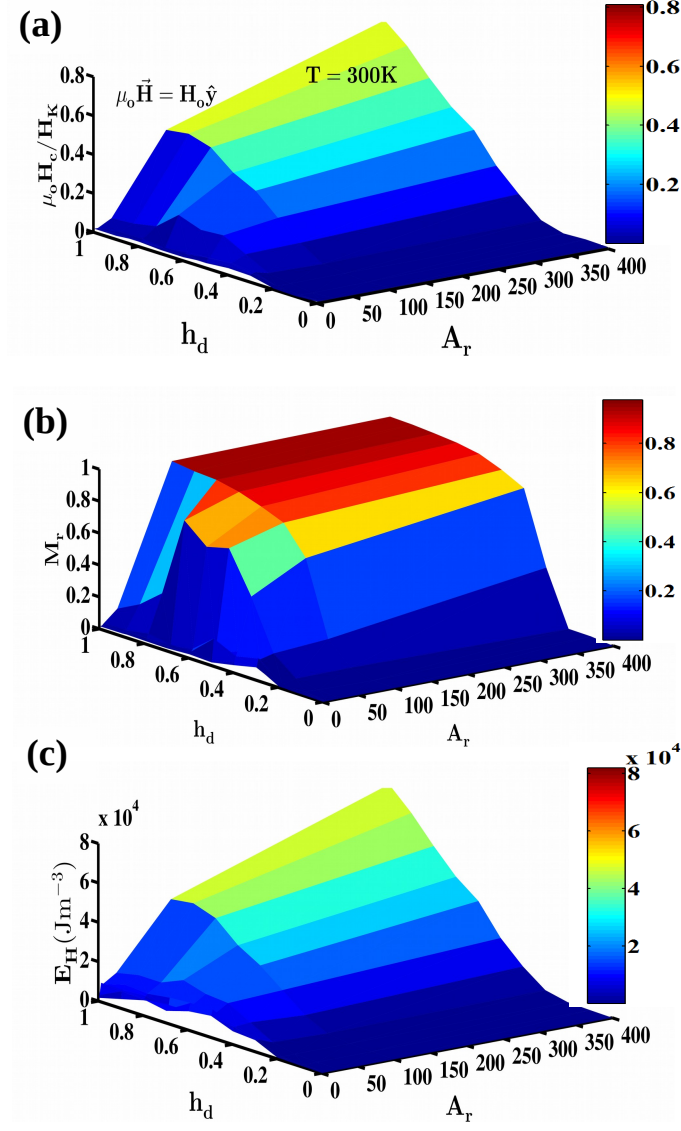


FIG. 9. Variation of the coercive field $\mu_o H_c$ (scaled by single-particle anisotropy field H_K), remanence M_r and hysteresis loop area E_H as a function of dipolar interaction strength h_d and aspect ratio A_r . The magnetic field is applied along the y -direction, and temperature T is taken as 300 K. For small aspect ratio and appreciable h_d , $\mu_o H_c$ and M_r have negligible values. There is an increase in value of $\mu_o H_c$ and M_r with an increase in h_d , indicating ferromagnetic behaviour. Interestingly, the variation of E_H with h_d and A_r is the same as that of coercive field variation.

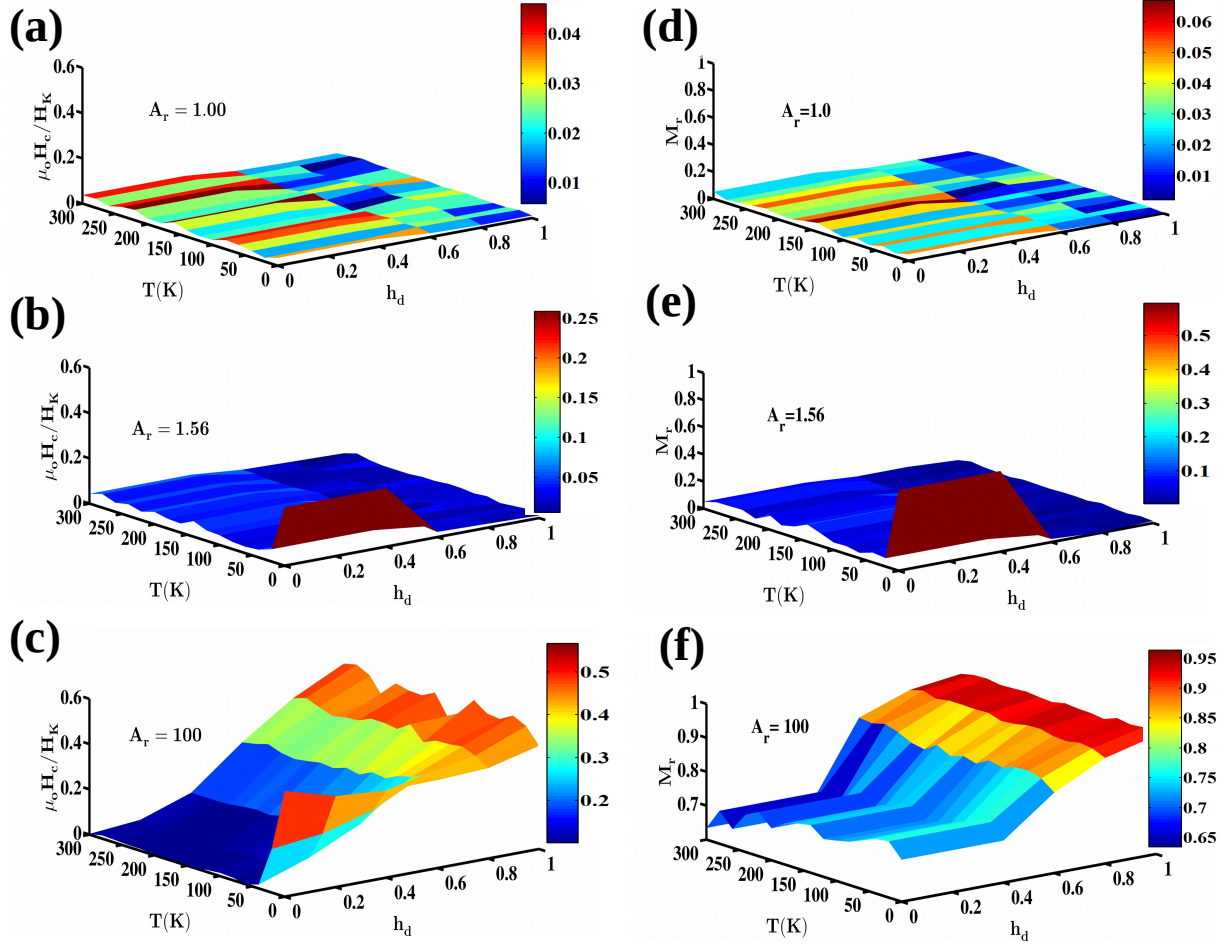


FIG. 10. Variation of the coercive field $\mu_o H_c$ (scaled by H_K) and remanence M_r as a function of temperature T and dipolar interaction strength h_d for three representative values of aspect ratio $A_r = 1.0, 1.56$ and 100 . Irrespective of T and h_d , $\mu_o H_c$ and M_r is negligibly tiny for square sample ($A_r = 1.0$). Even in the case of $A_r = 1.56$, there is a weak dependence of $\mu_o H_c$ and M_r on T and h_d except at small temperature and dipolar interaction strength. Interestingly, there is an increase in $\mu_o H_c$ and M_r with h_d for a fixed temperature. There is a rapid fall in these values with temperature for weak dipolar interaction strength. While for sizeable dipolar interaction, there is a weak dependence of coercive field and remanence on temperature.